

Concentration and localization of co-expressed ELAV/Hu proteins control specificity of mRNA processing

**EMANUELA ZAHARIEVA^{1†*}, IRMGARD U. HAUSSMANN^{1,2*}, ULRIKE BRÄUER¹
AND MATTHIAS SOLLER^{1,3}**

¹School of Biosciences, College of Life and Environmental Sciences, University of Birmingham, Edgbaston, Birmingham, B15 2TT, United Kingdom

²Department of Applied Science and Health, Faculty of Health and Life Sciences, Coventry University, Coventry, CV1 5FB, United Kingdom

Running Title: ELAV/Hu RNA binding proteins can share targets

Key Words: ELAV/Hu family proteins, alternative splicing/polyadenylation, neuron-specific RNA binding protein, ELAV-regulated genes, sex determination and dosage compensation

*equal contributing authors

³ Corresponding author

Matthias Soller

School of Bioscience

College of Life and Environmental Sciences

University of Birmingham

Edgbaston

Birmingham B15 2TT

Tel #: 0121 414 59 05

FAX #: 0121 414 59 25

m.soller@bham.ac.uk

† present address: Department of Neurobiology, Northwestern University, Evanston Il, USA

Abstract

Neuronally co-expressed ELAV/Hu proteins comprise a family of highly related RNA binding proteins, which bind to very similar cognate sequences. How this redundancy is linked to in vivo function and how gene specific regulation is achieved, has not been clear. Analysis of mutants in *Drosophila* ELAV/Hu family proteins ELAV, FNE and RBP9, and genetic interactions among them, indicates mostly independent roles in neuronal development and function, but convergence in the regulation of synaptic plasticity. Conversely, ELAV, FNE, RBP9 and human HuR bind ELAV target RNA in vitro with similar affinity. Likewise, all can regulate alternative splicing of ELAV target genes in non-neuronal wing-disc cells and substitute ELAV in eye development with artificially increased expression, but can also substantially restore ELAV's biological functions, when expressed under the control of the *elav* gene. Furthermore, ELAV related Sex-lethal can regulate ELAV targets and ELAV/Hu proteins can interfere with sexual differentiation. An ancient relationship to Sex-lethal is revealed by gonadal expression of RBP9 providing a maternal failsafe for dosage compensation. Our results indicate that highly related ELAV/Hu RNA binding proteins select targets for mRNA processing based on expression levels and sub-cellular localization, but only minimally by altered RNA binding specificity.

Introduction

RNA binding proteins (RBPs) are key regulators of gene expression. Through regulation of alternative splicing and polyadenylation, they expand the proteome and control spatio-temporal expression by affecting mRNA transport, turn-over, localization and translatability (16, 25). In the brain, alternative mRNA processing is particularly abundant and substantially contributes to the complexity of this organ (12, 56). Many RBPs comprise highly related gene families, but they seem to discriminate only marginally between short cognate binding sequences (46). Although redundancy can be evolutionary stable over extended periods of time (24), it is not clear if highly related RBPs act redundantly *in vivo* regulating mostly the same genes in the same biological process, or if they have diverged such that they regulate genes involved in different biological processes. Detailed analysis of the functions of highly related RBPs in animal models is required to decipher the underlying mechanisms how highly related RBPs achieve target specificity.

ELAV (Embryonic Lethal Abnormal Visual system)/Hu proteins comprise a family of RBPs broadly co-expressed in the nervous system and widely used neuronal markers (22, 59). ELAV/Hu proteins are proto-type RBPs, which harbor three highly conserved RNA Recognition Motifs (RRMs), whereby the first two RRM are arranged in tandem and the third RRM is separated by a less conserved hinge region. Humans have four *ELAV/Hu* genes (*HuB*, *HuC*, *HuD* and *HuR*), while *Drosophila* has three (*elav*, *fne* and *Rbp9*), which derive from a common ancestor, but have duplicated independently in vertebrates and arthropods (51). In mice, all Hu proteins are expressed in largely overlapping patterns in mature neurons (39). In addition, HuB is also expressed in gonads and HuR is ubiquitous. Expression of ELAV and FNE in *Drosophila*

starts with the birth of neurons, while RBP9 is first detected in late larval neurons (27, 52, 73). RBP9 is also expressed in gonads. The closest relative of ELAV family proteins in flies is Sex-lethal (Sxl), the master regulator of sexual differentiation and dosage compensation (54).

Due to its nuclear localization, the founding member of the ELAV/Hu family of RBPs, *Drosophila* ELAV, has initially been associated with gene-specific regulation of alternative splicing and polyadenylation, but can also regulate mRNA stability (30, 32, 37, 48, 55, 60, 64). Human Hu RBPs have on the contrary mostly been associated with regulating stability of mRNAs, their localization and translatability, but were recently also shown to regulate alternative pre-mRNA processing (2, 5, 23, 35, 38, 68, 75, 76). Although ELAV/Hu family RBPs bind to short, uridine-rich motives, which are ubiquitously found in introns and untranslated regions, they seem to have a complement of dedicated target genes (23, 35, 38, 68) and their activities are not restricted to a specific process in the life of an mRNA (59). Since ELAV/Hu RBPs can shuttle between the nucleus and cytoplasm (15), they likely also exert gene-specific functions depending on cellular localization.

Although ELAV family RBPs are broadly co-expressed in the brain of *Drosophila*, initial characterization of mutants of individual *elav* family genes revealed a number of distinct developmental and behavioral phenotypes. *elav* is required for axonal targeting in the embryonic central nervous system (CNS), synaptic growth, photoreceptor survival and neuronal migration in the optic lobe (8, 19, 55), and *fne* for mushroom body development and male courtship performance (74), while *Rbp9* supports blood brain barrier integrity and extended life span of flies (26, 66). Since these phenotypes have not comprehensively been analysed in mutants of all *elav* family genes, or in combinations thereof, it has not been clear, if and to what extent they have overlapping functions. Our results indicate that ELAV family RBPs in *Drosophila* exert

specific functions in the development, maintenance and functioning of the nervous system, but that they converge in the regulation of synaptic growth in ELAV and FNE/RBP9 independent pathways. Intriguingly, however, FNE, RBP9, human Hu RBPs and closely related Sxl, can regulate alternative splicing of ELAV target genes in non-neuronal wing disc cells, and all ELAV's can direct eye development by GAL4/UAS mediated artificially increased expression. When placed under the control of the *elav* promoter and UTRs, they can substitute for ELAV function at an organismal level. ELAV/Hu RBPs can also interfere with sexual differentiation and an ancient relationship to Sxl is revealed by gonadal expression of RBP9 providing a maternal failsafe for dosage compensation by the male-specific lethal (MSL) complex. Since ELAV/Hu RBPs bind RNA rather in discriminatively and can substantially rescue *elav* mutants under the regulatory control of the *elav* gene, these results indicate that selection of target genes is mainly achieved through alteration of expression levels and sub-cellular localization, but only marginally by altered RNA binding specificity.

Materials and Methods

Fly genetics and recombinant DNA technology

Fly breeding, genetics and recombinant DNA technology were done according to standard procedures as described (61). The *fne* null allele, *fne*^Δ, was generated by FLP/FRT mediated recombination between the following two transposon insertion lines, *PBac{WH}fne*^{f06439} and *PBac{WH}hec*^{f06077} (Supplemental Fig S2) (41, 63). Whole eye clones of *elav*^{e5} null allele were generated as described (62) using an *elav*^{e5} *w FRT19B* chromosome. Larvae and adult animals were obtained by using the *elav*^{ts1} temperature-sensitive allele transheterozygous with *elav*^{e5} and reared at the permissive temperature (18° C) for 3 days and then shifted to the restrictive temperature (25° C). To avoid unrelated effects from the genetic background of homozygously viable alleles, they were out-crossed to a lethal allele in the case of *elav*, or to small chromosomal deficiencies *Df(1)ED7165* for *fne* or *Df(2L)ED206* for *Rbp9*. Further details about mutant alleles and gene expression patterns can be found in Flybase (www.flybase.org). Transgenic flies were obtained by phiC31 mediated transformation as described (17) using landing sites at 57F (RBP9 genomic construct, *PBac{y⁺-attP-3B}VK22*), 76A (*UAS* constructs, *PBac{y⁺-attP-3B}VK00002*) and 55C (genomic rescue constructs, *P{y[+t7.7]=CaryP}attP1*). The additional *UASHAelav* construct was inserted in 86F (*M{3xP3-RFP.attP'}ZH-86Fa*). The 3xmyc epitope-tag was cloned into Pacman CH322-140N12, which contains a genomic fragment encompassing the entire *Rbp9* gene, by using the two BamHI sites harbored in the beginning of the N-terminal auxillary domain of *Rbp9* generating the following sequence (AGCACCACCGGATCaggagaacaaaattaatttcagaagaagacttaagtactgagcagaagctaataagcgaggagga

tctatccggagaacaaaaattaatttcagaagaagacTTACCGGCTACGGCC). The genomic region of the *fne* gene was obtained by PCR amplification of a modified pUC containing an attB site for integration and a GFP marker for identification of transgenic flies using primers pUC P *fne* F (cccgaaagtgaagtgaaagcattttgcgacgcctcccgaagctacacccgaaaatcaactccaacGACAGAATTCGAG TTCAAGAAGAAGGCG) and pUC P 3xP3 *fne* R (ccttggaaataccaatgtcaactttggttcaaggccaccagcagtcggtggaagactccaccaagacgtcCCGGCGGCC GCGTCTAGATAACTTCG), and then retrieval from the Bac clone RP98-39D14 by recombineering according to the manufacturer's protocol (GeneBridges). A 2x hemagglutinin (HA) tag was then inserted using NcoI and BamHI sites into the N-term of FNE generating the following sequence (ACCAACGCCATGgcaagtactaccctacgacgtgcccgactacgcccagggaggtaccctacgacgtgcccgactacgcccgATATTGTGAAGA). UAS constructs were generated by cloning the open reading frames (ORF) into *pUASTMSattB*, which contains a modified polylinker and an *attB* site inserted between the BamHI and SphI sites before the UAS promoter, and an *SV40* trailer. In addition, a 29 nt translation initiation site from the *adh* gene (gaattcgagatctaaagagcctgctaaagcaaaaaagaagtcacc), followed by the following start sequence (atgtcgaccggctcgagc) and a 2x hemagglutinin (HA) tag were introduced before the ORF and 60 nts of the *elav* UTR following the stop codon were also added to *UASHAelav* constructs, but these 60 nts were omitted from other *UAS* constructs. To generate the *UASHAfne*, *UASHARBP9* and *UASHAHu* constructs the *elav* ORF was swapped using flanking HindIII and XbaI sites, and an additional SphI site in the vector to set up a three-way ligation. To express Sxl and Halfpipe (Hfp), *UAS* transgenes on the 2nd and 3rd chromosomes, and for B52 on the 2nd chromosome were used (33, 45, 53). Genomic rescue constructs were cloned into a modified *pCaSpR* containing the

elav promoter (19) and modified to start with the ATG after exon 2 of *elav*. An HA tag was inserted in frame after amino acid nine of *elav* flanked by a EcoRI and SgrAI sites (attccaTACCCCTACGACGTGCCCGACTACGCCgcc), followed by the ORF starting with the first aa after the ATG, an AscI site generated by transformation of the sequence after the stop codon, 1176 nts of the *elav* 3'UTR including the NheI site and an *attB* site. For the *elavNLSHARBP9* construct, an NLS sequence (ggcGTGAGCCGCAAGCGCCCCCGCCCCGGCcca) was inserted after amino acid eight of *elav* before the HA tag using EcoRI and SgrAI sites (72). The *eFVGU* construct was generated by swapping the *ewg* ORF and UTR as in *eFeG* (19) with the *elav* ORF and UTR as described above using the NheI and EcoRI sites in *eFeG*.

EMSAs, RT-PCR, protein and Western analysis, antibody stainings and histology

Production of recombinant proteins, ³²P labeled *in vitro* transcripts and EMSAs were done as described (61). RNA extraction and RT-PCR was done as described (61). Polyacrylamide gels were dried, exposed to phosphoimager screens (BioRad) and quantified with QuantityOne (BioRad). cDNAs from *ewg* transcripts were amplified with primers *ewg4F* and *ewg5R*, *ewg6F* and *ewg6R*, from *nrg* using primers *nrg2F*, *nrg2S* and *nrg3L*, and from *arm* using primers *armF* and *armR* (31, 60). Protein gels and Western analysis were done according to standard protocols as described (Soller 2005) using rat anti-ELAV antibody (MAb 7E8A10, DHSB, 1:250), rat anti-HA antibody (3F10, Roche, 1:50) and mouse anti-alpha-tubulin (Sigma, 1;100,000). In situ antibody stainings were done as described (19), using rat anti-HA (MAb 3F10, Roche, 1:20), mouse anti-*elav* (MAb 7D, DHSB, 1:20, which recognizes 7 aa unique to ELAV, (36)), mouse anti FasII (1D4, DHSB, 1:100), MAb BP102 (DHSB, 1:20), anti-GFP (Molecular probes, 1:500)

and visualized with Alexa488- and/or Alexa647-coupled secondary antibodies (Molecular probes, 1:250), or by diaminobezidine staining (1 mg/ml) in the presence of 0.01 % H₂O₂ using horseradish peroxidase coupled secondary antibodies (Sigma, 1:10,000). DAPI was used at 1 µg/ml. Paraffin sections were done as described (57).

For quantification of antibody stainings in wing imaginal discs, the full width of at least four discs per genotype were scanned and fluorescence intensity quantification was done on the average Z-series projection of the stack in ImageJ, as previously described by (65).

For imaging of larval and adult brains confocal Z stacks were taken using the 40x objective lens on a Leica SP5/SP2 at multiple positions to ensure the complete capture of the imaged brain with sufficient spatial overlap in between each position. The number of Z stacks and acquisition settings were kept constant for each brain that was being imaged. The average intensity overlay from the stacks was stitched together using the FIJI 2D stitching plugin using ImageJ (43).

Behavioral analysis, longevity and statistics

Negative geotaxis assay was performed as described (11). Briefly, 20 adult flies per genotype were anesthetized with CO₂, placed in a bottom closed 25 ml plastic pipette and left to recover for 30 minutes. Flies were tapped to the bottom of the column and left to climb up for 45 sec. The number of flies that climbed above the 25 ml mark (n_{top}) and the ones remaining below the 2 ml (n_{bottom}) were recorded. Recovery time between repeats was 1 minute. A performance index (PI) was calculated as follows: $PI = 0.5 \times (n_{\text{total}} + n_{\text{top}} - n_{\text{bottom}}) / n_{\text{total}}$. Statistical analysis was done by ANOVA followed by planned pairwise comparisons using Fisher's protected least significance difference using StatView.

For the analysis of longevity, 60 flies per genotype were aged for 60 days in groups of 20 per vial without live yeast. Viable flies were transferred to fresh food media every three-five days and dead flies were recorded.

Results

Highly related and co-expressed *Drosophila* ELAV family RNA binding proteins exert distinct biological functions, but converge in the regulation of synaptic growth

Drosophila ELAV family RBPs are neuronally co-expressed and are highly homologous in their RNA binding domains ranging in similarity from 90-93% in RRM1, 76-90% in RRM2 and 90-98% in RRM3 (Supplemental Table S1). Compared to human Hu RBPs they share 84-91%, 76-82% and 84-90% similarity in RRMs 1-3, respectively. Although expression patterns of ELAV, FNE and RBP9 had been determined individually, there is only limited information about their overlapping expression (27, 52). Since we were unable to obtain highly specific antibodies for FNE and RBP9, we generated epitope-tagged genomic constructs to assess their co-expression. Analysis of the expression from these constructs in transgenic flies and comparison with the expression pattern of ELAV revealed that FNE and ELAV, as well as RBP9 and ELAV are co-expressed in all neurons in the adult brain (Supplemental Fig S1). ELAV is mostly nuclear, FNE about equally distributed between nucleus and cytoplasm, and RBP9 is mostly cytoplasmic (Supplemental Fig S1). To determine the extent of highly homologous ELAV family RBPs in acting redundantly in *Drosophila*, we analyzed mutants of *elav* (*elav^{e5}* null and *elav^{ts1}* temperature-sensitive alleles, (73)), *fne* (null allele, Supplemental Fig S2) and *Rbp9* (*Rbp9^{P2690}* null allele, (28), and combinations thereof for developmental and behavioral phenotypes assigned to one of the ELAV family gene in mutants of the other two (Figs 1A-AD) (8, 19, 26, 55, 66, 74).

The *elav^{e5}* null mutant is embryonic lethal, while *fne^Δ* and *Rbp9^{P2690}* null mutants, or *fne^Δ*; *Rbp9^{P2690}* double mutants are viable. Raising *elav* temperature-sensitive mutants (*elav^{e5}/elav^{ts1}*)

during embryogenesis at the permissive temperature renders them weakly adult viable (23 %). Double mutants of *elav^{e5}/elav^{ts1}* with either *fne^Δ* or *Rbp9^{P2690}* results in larval/pupal lethality and triple mutants are embryonic lethal. Mutants of *elav^{e5}* exert defects in axonal wiring during embryonic nervous system development resulting in irregular positioning of neuromeres and thinning of commissures and connectives, but this phenotype does not worsen in *elav^{e5} fne^Δ* double null or *elav^{e5} fne^Δ; Rbp9^{P2690}* triple null mutant combination (Figs 1A-D) arguing for a unique function of *elav* in this process.

Next, we analyzed *elav* family mutants and combinations for defects in synaptic growth at third instar neuromuscular junctions (NMJs, Figs 1E-L). Here, a strong reduction in the number of synaptic connections is observed in *elav^{e5}/elav^{ts1}* mutants, which does not significantly decrease in the absence of *fne* and *Rbp9* (Figs 1I, 1J and 1L). Mutants of *fne^Δ* and *Rbp9^{P2690}* have a slightly reduced and slightly increased numbers of synaptic boutons, respectively, but strikingly, *fne^Δ; Rbp9^{P2690}* double mutants show a dramatic reduction of synaptic connections suggesting that they act in the same pathway (Figs 1K and 1L). The lack of genetic interactions of *elav* with *fne* and *Rbp9* further suggests that they regulate synaptic growth independently.

For the development of adult mushroom bodies, *fne* is required for restricting axonal extension of the beta lobe (74), but this phenotype was not observed in *elav^{e5}* or *Rbp9^{P2690}*, and did not get worse in *fne^Δ; Rbp9^{P2690}* double mutants (Figs 1M-Q) indicating a unique function of *fne* in this process.

During pupal development, *elav* is required for rotation of the medula, and in adult flies for maintenance of photoreceptor and central brain neurons (Figs 1R-AB, (8). These phenotypes were not observed in *fne^Δ*, *Rbp9^{P2690}* and *fne^Δ; Rbp9^{P2690}*, except for occasional vacuolizations observed in the lamina of *fne^Δ; Rbp9^{P2690}* double mutants (10 out of 12). Furthermore,

elav^{e5}/elav^{ts1} mutants had a much more dramatically reduced lifespan than *fne^Δ*, *Rbp9^{P2690}* and *fne^Δ; Rbp9^{P2690}* mutants (Fig 1AC), but the lack of a genetic interaction between *fne* and *Rbp9* suggests non-overlapping functions. Similarly, adult locomotion as assayed with a negative geotaxis assay was impaired in an age-dependent manner in *Rbp9^{P2690}*, but not in *fne^Δ* (Fig 1AD) eluding overlapping functions. In contrast, *elav^{e5}/elav^{ts1}* mutants showed much more reduced locomotion and were also ataxic (Fig 1AD).

Taken together, individual ELAV family genes have mostly distinct roles during neuronal development, maintenance and function shown by the absence of genetic interactions, but convergence in the regulation of synaptic plasticity.

Alternative splicing of known ELAV targets is unaffected in *fne^Δ; Rbp9^{P2690}* null mutants

The major target of ELAV, *ewg*, has a prominent function in regulating synaptic growth at third instar NMJs (18, 19). Since FNE and RBP9 also affect this process, we wondered if FNE and RBP9 regulate alternative splicing of the ELAV target genes *ewg*, *nrg* and *arm* in a subset of *Drosophila* neurons. Although in the absence of ELAV, the neuronal isoforms of these genes are completely absent in photoreceptor neurons (32, 58), this analysis has not been comprehensively extended to all parts of the brain leaving the possibility that FNE and/or RBP9 could assist or substitute ELAV in the regulation of these genes. No obvious reduction in the neuronal isoform of these three genes was detected in *fne; Rbp9* double mutants by RT-PCR from adult brains (Fig 2A). Potentially, loss of FNE and RBP9 could affect alternative splicing only in a few cells in the brain, which would not be detected by RT-PCR. To visualize alternative splicing at a cellular resolution, we used a *nrg* GFP reporter (*UNGA*, (64), Fig 2B) which is ELAV-dependent (Fig 2C and D). In the absence of FNE and RBP9, all neurons expressing ELAV also alternatively

splice the *nrg* GFP reporter UNGA in larval photoreceptor neurons, and in larval and adult brains (Fig 2E-I), which was also observed in photoreceptor neurons and larval brains of individual mutants of *fne* or *Rbp9* (Supplemental Fig S3).

Recombinant FNE, RBP9 and HuR bind to ELAV target RNA with similar affinities

Next, we determined the RNA binding specificity of ELAV family members *in vitro* using the well-characterized ELAV binding sequence in the *ewg* gene (pA-I), which comprises 135 bp (17, 60, 61). For these binding experiments, we generated recombinant proteins in *E. coli* for ELAV, FNE and RBP9, but also for human HuR, because it is functionally closest to ELAV family proteins in *Drosophila* (Fig 3A, Supplemental Fig S4 and Supplemental Table 1). Surprisingly, all proteins bound *ewg* pA-I RNA in a narrow affinity range and also cooperatively formed multimeric complexes similar to ELAV in electrophoretic mobility shift assays (EMSA, Figs 3B and C). Multimeric complexes of rFNE and rHuR assembled on pA-I RNA run faster in accordance with their size (Figs 3A and B), which has previously been observed with the N-terminally truncated form of ELAV, RBD60 (73). Binding constants for rELAV, rFNE, rRBP9 and rHuR were 22 nM, 47 nM, 23 nM and 49 nM, respectively (Fig 3C).

FNE, RBP9 and Hu proteins can regulate alternative splicing of ELAV target genes

Expression of ELAV in non-neuronal wing discs results in neuronal splicing of ELAV target genes (32). Since recombinant FNE, RBP9 and HuR bound ELAV target RNA with similar affinities, we wanted to know if they could also regulate *elav* target genes when expressed in wing discs. ELAV family RBPs were expressed from hemagglutinin-tagged (HA) *UAS* transgenes (Fig 4A). Expression in non-neuronal wing-disc tissue using *dppGAL4* results in

neuronal splicing of *ewg*, *nrg* and *arm* using RT-PCR or the *UNGA* reporter, respectively (Figs 4B and 4C-G). The more distantly related poly-U RBP Halfpipe (Hfp) or the SR protein B52 did not induce alternative splicing of the *nrg* reporter *UNGA* (Figs 4H and I). Consistent with a role in alternative splicing regulation, ELAV and HuR predominantly localize to the nucleus. FNE showed no distinct localization, while RBP9 was predominantly present in the cytoplasm (Figs 4J-M). Expression of HuB and HuC from *UAS* transgenes with *dppGAL4* promoted neuron-specific splicing of *UNGA* (Supplemental Figure S4), but HuD was not detectable and did not induce GFP expression, although expression with *elavGAL4^{c155}* resulted in lethality. Since expression of HuB and HuC was also undetectable or resulted in lethality with some neuronal *GAL4* drivers, we focused on HuR.

Ectopic expression of all ELAV/Hu family RBPs in non-neuronal wing discs induced neuron-specific alternative splicing of the known ELAV targets and they behaved indiscriminately likely due to expression levels saturating for *UNGA* regulation (Fig 4T, 25°C). To reduce concentrations of ELAV/Hu RBPs a temperature-sensitive inhibitor of GAL4 expressed under a *UAS* promoter, *UASGAL80^{ts}*, was used. This genetic configuration resulted in reduced expression of ELAV and concomitant neuronal alternative splicing of the *UNGA* reporter at 25°C (Figs 4N-T). At this temperature, FNE and RBP9 were not able to induce the *UNGA* reporter, while induction by HuR was comparable to ELAV (Figs 4O, S and T) indeed revealing different thresholds in vivo.

FNE, RBP9 and Hu proteins can partially substitute ELAV in eye development

Since FNE, RBP9 and HuR can regulate alternative splicing of ELAV target genes we wanted to know whether they could substitute ELAV in eye development, as broader expression interferes

with organismal viability. For this experiment, we used an *elav* flip-out rescue construct, *eFVGU*, where the ELAV ORF is flanked with *FRT* sites followed by *GAL4* leading to artificially increased expression. When *elav* is removed with *eyflp* in the eye-primordium, GAL4 will be expressed, which can then drive *UAS* transgenes (Fig 5A). In the absence of ELAV only a tiny eye developed (Figs 5B-D). In contrast, the presence of ELAV, FNE, RBP9 or HuR, but not ELAV's closest relative Sex-lethal (*Sxl*), rescued eye development substantially (Figs 5E-P). Pan-neural expression of ELAV with the GAL4 *UAS* system, however, was unable to rescue viability of *elav* null mutants.

FNE, RBP9 and HuR rescue ELAV function under endogenous control of the *elav* gene

Mutants of ELAV family RBPs in *Drosophila* show distinct phenotypes, but the proteins showed little discrimination at the level of RNA binding or ELAV target gene regulation, when overexpressed. We therefore reasoned that distinct functions of these proteins are tightly linked to their expression levels. Indeed, during embryogenesis and larval life, ELAV is the dominantly expressed ELAV family protein. In contrast, FNE and RBP9 expression is high during pupal development and RBP9 shows predominant expression in adults (Supplemental Fig S5). Since the GAL4/*UAS* system leads to increased and also delayed expression we wanted to more accurately test if distinct functions depend on expression levels. Therefore, we exchanged the ELAV ORF in an HA-tagged *elav* rescue construct harboring its UTRs with the ORFs coding for FNE, RBP9 and HuR (Fig 6A) and inserted these constructs into the same genomic locus resulting in the same expression levels. Expression of RBP9 and HuR in these transgenic flies was comparable with expression of ELAV, while FNE seems to be less stable (Fig 6B). The *elav^{HAELAV}* transgene rescued viability of the strong hypomorphic allele *elav^{ts1}* (Fig 6C).

Strong rescue was also obtained with *elavHAHuR*, while *elavHARBP9* and *elavHAFNE* rescued less good. Although only the *elavHAHuR* transgene showed a marginal rescue of the *elav^{es}* null allele (5 % with two copies, n=100), all four transgenes rescued synaptic growth defects when *elav^{es}/elav^{ts1}* animals were raised at the permissive temperature during embryonic development (Fig 6D). Since RBP9 rescued less than HuR, cellular localization could be the reason for this. RBP9 localized predominantly to the cytoplasm, while HuR was predominantly nuclear and FNE was equally present in the nucleus and cytoplasm (Figs 6E-P). When RBP9 was targeted to the nucleus by including an NLS in the transgene (Fig 6Q), the *elavNLSHARBP9* transgene rescued *elav^{ts1}* comparably to *elavHAELAV* (Fig 6C), but did not rescue the *elav^{es}* null allele (n=498). Accordingly, nuclear localization is increased in all neurons. In a subset of neurons, however, NLSRBP9 was predominantly nuclear, while ELAV became cytoplasmic (Figs 6Q-S).

ELAV related Sxl can regulate alternative splicing of ELAV target genes and ELAV can interfere with sexual differentiation

The closest relative of ELAV family RBPs in flies is Sxl, which is the master regulator of sex determination and dosage compensation in *Drosophila*, but a neuronal protein in other Diptera (3, 49). Sxl has 63% and 64% similarity in RRM1 and RRM2, respectively (Supplemental Table S1), but does not have the third RRM implicated in multimerization, although multiple Sxl proteins bind co-operatively to target RNA (65, 71). We therefore asked, if Sxl can induce neuron-specific alternative splicing of the *UNGA* reporter in wing discs. Indeed, Sxl also induced neuron-specific alternative splicing of the *UNGA* reporter in wing discs (Figs 7A-C). Since Sxl is able to substitute ELAV, we next tested if ELAV/Hu family RBPs can interfere with Sxl's role in sexual differentiation. For this experiment, ELAV/Hu family RBPs

(ELAV, FNE, RBP9 and HuR) were expressed in the pattern of *doublesex* (*dsx*), the main effector for sexual differentiation (47). Expression of ELAV/Hu family RBPs with *dsxGAL4* yielded pharate adults, which showed no genital differentiation in both sexes and impaired development of male sex combs, but male pigmentation was not affected and flies looked otherwise normal when dissected from the pupal case (Figs 7D-I). Males expressing Hfp or B52 in the *dsx* pattern did not show impaired development of sex-specific features.

Maternal RBP9 provides a failsafe for Sxl mediated dosage compensation

When over-expressing ELAV, FNE and RBP9 from *UAS* transgenes with neuronal *elavGAL4^{C155}*, we noticed pupal lethality of males (Fig 7J). Similarly, over-expression of Sxl also resulted in male lethality. FNE and RBP9 over-expression was more effective in killing males suggesting that cytoplasmic localization is required for this effect. Accordingly, routing RBP9 to the nucleus by including a nuclear localization signal (NLSRBP) relieved sex-specific toxicity suggesting interference with Sxl's role in dosage compensation (Fig 7J, (54). Similarly, males were effectively killed when a cytoplasmically localized ELAV derivative was expressed (ELAV^{OH}, (72). We therefore reasoned that expression of RBP9 during oogenesis could cooperate with Sxl in translational suppression of *male-specific lethal-2* (*msl-2*) to prevent dosage compensation in the early embryonic stages of female development. Indeed, removing one copy of RBP9 during oogenesis in combination with zygotic heterozygosity for Sxl results in female lethality (Fig 7K). This effect is of maternal origin, since there is no bias in female numbers in the RBP9 stock and the reverse cross did not show female lethality. Also, female lethality was prevented in *Sxl/+* daughters of *Rbp9/CyO* mothers, when *msl-3*, another protein of dosage compensation complex (located on the third chromosome) was zygotically removed (104%

rescue, n=102). Thus, maternal provision of RBP9 provides a failsafe to prevent dosage compensation early in female development.

Discussion

Neuronally co-expressed ELAV/Hu family RBPs are like many other RBPs highly conserved and show little discrimination in binding short U-rich motifs *in vitro* (46). Similar results were obtained for *Drosophila* ELAV proteins (ELAV, FNE and RBP9) as well as for human HuR when using the extended ELAV binding site in the *ewg* gene. In this ELAV target RNA, a number of short U-rich motifs are interspersed along the 135 nt binding site, but they do not have a fixed position eluding RNA secondary structure to contribute to target selectivity (17, 60, 61). Likewise, when artificially expressed in non-neuronal larval wing disc cells or during eye development, ELAV/Hu proteins can regulate neuron-specific splicing of ELAV target genes and substitute for ELAV in eye development. The capacity to induce neuron-specific splicing events resides in a very narrow concentration range whereby ELAV has only a slightly lower threshold. Accordingly, exchanging the ELAV ORF with other ELAV/Hu RBPs in the *elav* gene can substantially substitute for ELAV function in transgenic *Drosophila*, but also requires nuclear localization.

Concentration and localization of ELAV/Hu family proteins direct specificity of mRNA processing

Our data show that expression levels and cellular localization of ELAV/Hu proteins are important determinants for selection of target genes. Accordingly, broad over-expression of ELAV or other RNA binding proteins is lethal or results in developmental defects likely due to global mis-regulation of mRNA processing (33, 34). Functional significance of tissue-specifically increased concentrations for alternative splicing has been shown for a number of

RNA regulatory proteins (14, 44, 69). Also, quantitative variations of SR proteins and antagonistic hnRNP proteins have been shown to affect selection of alternative splice sites (7, 9). Importance in the control of expression of ELAV family proteins is further indicated by the complexity of their genes in *Drosophila*. They are about 10-15 times bigger than the average *Drosophila* gene, have several promoters and most prominently, have unusually long 3'UTRs (21, 50). Complex transcriptional control and extended UTRs are also found in Hu genes suggesting that elaborate regulation of expression of ELAV/Hu genes is a key features to exert their functions (6).

In addition, ELAV/Hu proteins have also been found to cross-regulate each other. ELAV controls 3'UTR extension by suppression of 3'end processing at proximal polyA sites in its own gene, but also in *fne* and *Rbp9* (20, 60). Cross-regulation is also found in HuD, where Hu proteins regulate inclusion of an alternatively spliced exon (70). Furthermore, RBP9 and Sxl are required for translational repression of *msl-2* to prevent dosage compensation of the X chromosome in female embryos revealing an ancient relationship between the two proteins. Intriguingly, in flies more distantly related to *Drosophila* such as the housefly *Musca*, Sxl is a neuronal protein, but is not required for sex determination and dosage compensation (3, 49).

ELAV/Hu RBPs have both nuclear and cytoplasmic functions in mRNA processing. Hence, differential sub-cellular localization e.g. by phosphorylation provides an additional level to regulate target selection (4). ELAV localizes predominantly to the nucleus and nuclear localization is required for viability (72), while RBP9 is predominantly cytoplasmic and FNE about equally distributed between the nucleus and cytoplasm. Given the pre-dominant localization of RBP9 to the cytoplasm, its capacity to regulate splicing in the nucleus is

unexpected, but could be explained by shuttling between the nucleus and the cytoplasm, which has been described for human Hu proteins (Fan and Steitz, 1998).

Distinct roles of *Drosophila* ELAV proteins in neuronal development and function, but convergence in synaptic plasticity

Mutants in the genes coding for ELAV family RBPs in *Drosophila* exert mostly distinct phenotypes in nervous system development, maintenance and function, but all of them show synaptic growth defects. Except for *fne* and *Rbp9* in synaptic growth regulation, no genetic interactions were detected leading to more severe developmental phenotypes. Double mutants for *fne; Rbp9* have less synaptic boutons than individual mutants, which is exactly what we would expect if they have overlapping functions. Since *fne* and *Rbp9* did not genetically interact with *elav*, they seem to act independently of *elav* in synaptic growth regulation. Further, the overlapping roles of *fne* and *Rbp9* seem specific to the regulation of synaptic growth, since locomotion and life span phenotypes, which assess neuronal function more broadly, were similar in single and double mutants.

Although *elav fne; Rbp9* triple mutants die as embryos and *elav fne* and *elav; Rbp9* double mutants as late larvae, no genetic interactions were observed for any developmental phenotype. The lethality of these mutant combinations is likely due to the general weakness of *elav* mutants. Determination of the target genes of *Drosophila* ELAV family RBPs in the future will reveal, if they have overlapping roles in regulating neuronal function more broadly.

ELAV/Hu protein regulated mRNA processing plays a major role in synaptic plasticity

Although ELAV in *Drosophila* is expressed as soon as neurons are born, it is mostly not required for neuronal development with the exception of a minor role in axonal wiring. The severe locomotion defects, including ataxia, of *elav* mutants suggest that ELAV is required in neurons for proper function or refining neuronal connections. Indeed, the major target of ELAV, *erect wing* (*ewg*), regulates the number of synaptic connections made (18, 19). Essential roles in neuronal function have been found in HuC mutant mice. Here, synthesis of the neurotransmitter glutamate is affected, resulting in reduced neuronal excitability and impaired motor function (23). In contrast, HuD mutant mice have transient developmental defects in the cerebellum, reduced locomotion activity and learning defects (1). Most intriguingly, however, HuC; HuD double mutants have a much more severe neurological phenotype and die soon after birth suggesting overlapping functions (23). This is further supported by shared sets of target genes of HuC and HuD affecting glutamate synthesis and genes coding for synaptic proteins. Similar observations have also been made for highly related NOVA1 and 2 in mice, which share an extended set of target genes involved in synaptic functions (67).

Our analysis of mutants in *Drosophila* ELAV family proteins revealed a major role of these RBPs in regulating synaptic growth. The role of ELAV family RBPs in structural synaptic plasticity is reminiscent of regulating higher order brain functions, e.g. learning and memory. In accordance, HuD is up-regulated upon learning in mice and also regulates GAP43 mRNA required for learning and memory (42). It is thus conceivable that a major role of ELAV/Hu proteins is in altering neuronal plasticity, whereby different ELAV proteins are used to integrate multiple signals to regulate an overlapping set of target genes.

A model for regulating gene expression by highly related RNA binding proteins

The limited number of genes in higher eukaryotes requires elaborate regulatory networks to generate molecular, cellular and functional complexity. A key feature of such regulatory networks is the integration of multiple signals to generate a gene expression output as e.g. shown for the regulation of synaptic growth in *Drosophila* (18, 19). It is conceivable, that highly related RBPs can regulate the same genes via overlapping or identical binding sites. Differential control in regulating the concentrations, activity to bind RNA and cellular localization then serves to integrate cellular status via distinct signaling pathways (Fig 8). An alternative route to bind target genes has been suggested through recruitment at the promoter and deposition by elongating RNA PolII (29). Our data from using heterologous promoters for expressing of *ewg* and *nrg* reporters, however, argue against this possibility for these genes, but might affect a minority of large genes (17, 40, 65).

In summary, our results demonstrate that ELAV/Hu proteins can exert overlapping functions due to their conserved recognition of highly similar RNA sequences. Their target specificity, however, is tuned by regulating cellular concentration and localization. Increased levels of RNA binding proteins, including ELAV/Hu proteins have been found in many cancers illustrating the importance for tight control (9, 10, 13). Thus, alterations of the expression levels, activity or cellular localization of ELAV/Hu proteins has major implications for human health.

Acknowledgments

We thank Bloomington, Exelixis/Harvard and Kyoto stock centers, and S. Goodwin, J. Simpson, J. Kim, J. Horabin, H. Richardson and G. Toba for fly lines, M-L. Samson and Developmental Hybridoma Studies Bank for antibodies, flybase for RNAseq data, J. Colburn for discussions, and S. Vilain for comments on the manuscript. For this work we acknowledge funding from the BBSRC and the Wellcome Trust.

References

1. **Akamatsu, W., H. Fujihara, T. Mitsuhashi, M. Yano, S. Shibata, Y. Hayakawa, H. J. Okano, S. Sakakibara, H. Takano, T. Takano, T. Takahashi, T. Noda, and H. Okano.** 2005. The RNA-binding protein HuD regulates neuronal cell identity and maturation. *Proc Natl Acad Sci U S A* **102**:4625-30.
2. **Antic, D., N. Lu, and J. D. Keene.** 1999. ELAV tumor antigen, hel-N1, increases translation of neurofilament M mRNA and induces formation of neurites in human teratocarcinoma cells [In Process Citation]. *Genes Dev* **13**:449-61.
3. **Bopp, D., G. Saccone, and M. Beye.** 2014. Sex determination in insects: variations on a common theme. *Sex Dev* **8**:20-8.
4. **Brauer, U., E. Zaharieva, and M. Soller.** 2014. Regulation of ELAV/Hu RNA-binding proteins by phosphorylation. *Biochem Soc Trans* **42**:1147-51.
5. **Brennan, C. M., and J. A. Steitz** 2001. HuR and mRNA stability. *Cell Mol Life Sci* **58**:266-77.
6. **Bronicki, L. M., and B. J. Jasmin.** 2013. Emerging complexity of the HuD/ELAV14 gene; implications for neuronal development, function, and dysfunction. *RNA* **19**:1019-37.
7. **Caceres, J. F., S. Stamm, D. M. Helfman, and A. R. Krainer.** 1994. Regulation of alternative splicing in vivo by overexpression of antagonistic splicing factors. *Science* **265**:1706-9.
8. **Campos, A.-R., D. Grossman, and K. White.** 1985. Mutant alleles at the locus *elav* in *Drosophila melanogaster* lead to nervous system defects. A developmental-genetic analysis. *J. Neurogen.* **2**:197-218.

9. **Chen, M., C. J. David, and J. L. Manley.** 2012. Concentration-dependent control of pyruvate kinase M mutually exclusive splicing by hnRNP proteins. *Nat Struct Mol Biol* **19**:346-54.
10. **Cooper, T. A., L. Wan, and G. Dreyfuss.** 2009. RNA and disease. *Cell* **136**:777-93.
11. **Coulom, H., and S. Birman.** 2004. Chronic exposure to rotenone models sporadic Parkinson's disease in *Drosophila melanogaster*. *J Neurosci* **24**:10993-8.
12. **Darnell, R. B.** 2013. RNA protein interaction in neurons. *Annu Rev Neurosci* **36**:243-70.
13. **David, C. J., and J. L. Manley.** 2010. Alternative pre-mRNA splicing regulation in cancer: pathways and programs unhinged. *Genes Dev* **24**:2343-64.
14. **Ehrmann, I., C. Dalglish, Y. Liu, M. Danilenko, M. Crosier, L. Overman, H. M. Arthur, S. Lindsay, G. J. Clowry, J. P. Venables, P. Fort, and D. J. Elliott.** 2013. The tissue-specific RNA binding protein T-STAR controls regional splicing patterns of neurexin pre-mRNAs in the brain. *PLoS Genet* **9**:e1003474.
15. **Fan, X. C., and J. A. Steitz.** 1998. Overexpression of HuR, a nuclear-cytoplasmic shuttling protein, increases the in vivo stability of ARE-containing mRNAs. *Embo J* **17**:3448-60.
16. **Glisovic, T., J. L. Bachorik, J. Yong, and G. Dreyfuss.** 2008. RNA-binding proteins and post-transcriptional gene regulation. *FEBS Lett* **582**:1977-86.
17. **Hausmann, I. U., M. Li, and M. Soller.** 2011. ELAV-mediated 3'-end processing of ewg transcripts is evolutionarily conserved despite sequence degeneration of the ELAV-binding site. *Genetics* **189**:97-107.

18. **Hausmann, I. U., and M. Soller.** 2010. Differential activity of EWG transcription factor isoforms identifies a subset of differentially regulated genes important for synaptic growth regulation. *Dev Biol* **348**:224-30.
19. **Hausmann, I. U., K. White, and M. Soller.** 2008. Erect wing regulates synaptic growth in *Drosophila* by integration of multiple signaling pathways. *Genome Biol* **9**:R73.
20. **Hilgers, V., S. B. Lemke, and M. Levine.** 2012. ELAV mediates 3' UTR extension in the *Drosophila* nervous system. *Genes Dev* **26**:2259-64.
21. **Hilgers, V., M. W. Perry, D. Hendrix, A. Stark, M. Levine, and B. Haley.** 2011. Neural-specific elongation of 3' UTRs during *Drosophila* development. *Proc Natl Acad Sci U S A* **108**:15864-9.
22. **Hinman, M. N., and H. Lou.** 2008. Diverse molecular functions of Hu proteins. *Cell Mol Life Sci* **65**:3168-81.
23. **Ince-Dunn, G., H. J. Okano, K. B. Jensen, W. Y. Park, R. Zhong, J. Ule, A. Mele, J. J. Fak, C. Yang, C. Zhang, J. Yoo, M. Herre, H. Okano, J. L. Noebels, and R. B. Darnell.** 2012. Neuronal Elav-like (Hu) proteins regulate RNA splicing and abundance to control glutamate levels and neuronal excitability. *Neuron* **75**:1067-80.
24. **Kafri, R., M. Springer, and Y. Pilpel.** 2009. Genetic redundancy: new tricks for old genes. *Cell* **136**:389-92.
25. **Keene, J. D.** 2007. RNA regulons: coordination of post-transcriptional events. *Nat Rev Genet* **8**:533-43.
26. **Kim, J., Y. J. Kim, and J. Kim-Ha.** 2010. Blood-brain barrier defects associated with Rbp9 mutation. *Mol Cells* **29**:93-8.

27. **Kim, Y. J., and B. S. Baker.** 1993. The *Drosophila* gene *rbp9* encodes a protein that is a member of a conserved group of putative RNA binding proteins that are nervous system-specific in both flies and humans. *J Neurosci* **13**:1045-56.
28. **Kim-Ha, J., J. Kim, and Y. J. Kim.** 1999. Requirement of RBP9, a *Drosophila* Hu homolog, for regulation of cystocyte differentiation and oocyte determination during oogenesis. *Mol Cell Biol* **19**:2505-14.
29. **Kornblihtt, A. R.** 2005. Promoter usage and alternative splicing. *Curr Opin Cell Biol* **17**:262-8.
30. **Koushika, S. P., M. J. Lisbin, and K. White.** 1996. ELAV, a *Drosophila* neuron-specific protein, mediates the generation of an alternatively spliced neural protein isoform. *Curr Biol* **6**:1634-41.
31. **Koushika, S. P., M. Soller, S. M. DeSimone, D. M. Daub, and K. White.** 1999. Differential and inefficient splicing of a broadly expressed *Drosophila* erect wing transcript results in tissue-specific enrichment of the vital EWG protein isoform. *Mol Cell Biol* **19**:3998-4007.
32. **Koushika, S. P., M. Soller, and K. White.** 2000. The neuron-enriched splicing pattern of *Drosophila* erect wing is dependent on the presence of ELAV protein. *Mol Cell Biol* **20**:1836-45.
33. **Kraus, M. E., and J. T. Lis.** 1994. The concentration of B52, an essential splicing factor and regulator of splice site choice in vitro, is critical for *Drosophila* development. *Mol Cell Biol* **14**:5360-70.

34. **Labourier, E., H. M. Bourbon, I. E. Gallouzi, M. Fostier, E. Allemand, and J. Tazi.** 1999. Antagonism between RSF1 and SR proteins for both splice-site recognition in vitro and Drosophila development. *Genes Dev* **13**:740-53.
35. **Lebedeva, S., M. Jens, K. Theil, B. Schwanhausser, M. Selbach, M. Landthaler, and N. Rajewsky.** 2012. Transcriptome-wide analysis of regulatory interactions of the RNA-binding protein HuR. *Mol Cell* **43**:340-52.
36. **Lisbin, M. J., M. Gordon, Y. M. Yannoni, and K. White.** 2000. Function of RRM domains of *Drosophila melanogaster* ELAV: RNP1 mutations and RRM domain replacements with ELAV family proteins and SXL. *Genetics* **155**:1789-98.
37. **Lisbin, M. J., J. Qiu, and K. White.** 2001. The neuron-specific RNA-binding protein ELAV regulates neuroglial alternative splicing in neurons and binds directly to its pre-mRNA. *Genes Dev* **15**:2546-61.
38. **Mukherjee, N., D. L. Corcoran, J. D. Nusbaum, D. W. Reid, S. Georgiev, M. Hafner, M. Ascano, Jr., T. Tuschl, U. Ohler, and J. D. Keene.** 2012. Integrative regulatory mapping indicates that the RNA-binding protein HuR couples pre-mRNA processing and mRNA stability. *Mol Cell* **43**:327-39.
39. **Okano, H. J., and R. B. Darnell.** 1997. A hierarchy of Hu RNA binding proteins in developing and adult neurons. *J Neurosci* **17**:3024-37.
40. **Oktaba, K., W. Zhang, T. S. Lotz, D. J. Jun, S. B. Lemke, S. P. Ng, E. Esposito, M. Levine, and V. Hilgers.** 2015. ELAV links paused Pol II to alternative polyadenylation in the *Drosophila* nervous system. *Mol Cell* **57**:341-8.
41. **Parks, A. L., K. R. Cook, M. Belvin, N. A. Dompe, R. Fawcett, K. Huppert, L. R. Tan, C. G. Winter, K. P. Bogart, J. E. Deal, M. E. Deal-Herr, D. Grant, M.**

- Marcinko, W. Y. Miyazaki, S. Robertson, K. J. Shaw, M. Tabios, V. Vysotskaia, L. Zhao, R. S. Andrade, K. A. Edgar, E. Howie, K. Killpack, B. Milash, A. Norton, D. Thao, K. Whittaker, M. A. Winner, L. Friedman, J. Margolis, M. A. Singer, C. Kopczynski, D. Curtis, T. C. Kaufman, G. D. Plowman, G. Duyk, and H. L. Francis-Lang.** 2004. Systematic generation of high-resolution deletion coverage of the *Drosophila melanogaster* genome. *Nat Genet* **36**:288-92.
42. **Pascale, A., P. A. Gusev, M. Amadio, T. Dottorini, S. Govoni, D. L. Alkon, and A. Quattrone.** 2004. Increase of the RNA-binding protein HuD and posttranscriptional up-regulation of the GAP-43 gene during spatial memory. *Proc Natl Acad Sci U S A* **101**:1217-22.
43. **Preibisch, S., S. Saalfeld, and P. Tomancak.** 2009. Globally optimal stitching of tiled 3D microscopic image acquisitions. *Bioinformatics* **25**:1463-5.
44. **Qi, J., S. Su, M. E. McGuffin, and W. Mattox.** 2006. Concentration dependent selection of targets by an SR splicing regulator results in tissue-specific RNA processing. *Nucleic Acids Res* **34**:6256-63.
45. **Quinn, L. M., R. A. Dickins, M. Coombe, G. R. Hime, D. D. Bowtell, and H. Richardson.** 2004. *Drosophila* Hfp negatively regulates dmyc and stg to inhibit cell proliferation. *Development* **131**:1411-23.
46. **Ray, D., H. Kazan, K. B. Cook, M. T. Weirauch, H. S. Najafabadi, X. Li, S. Gueroussov, M. Albu, H. Zheng, A. Yang, H. Na, M. Irimia, L. H. Matzat, R. K. Dale, S. A. Smith, C. A. Yarosh, S. M. Kelly, B. Nabet, D. Mecnas, W. Li, R. S. Laishram, M. Qiao, H. D. Lipshitz, F. Piano, A. H. Corbett, R. P. Carstens, B. J. Frey, R. A. Anderson, K. W. Lynch, L. O. Penalva, E. P. Lei, A. G. Fraser, B. J.**

- Blencowe, Q. D. Morris, and T. R. Hughes.** 2013. A compendium of RNA-binding motifs for decoding gene regulation. *Nature* **499**:172-7.
47. **Rideout, E. J., A. J. Dornan, M. C. Neville, S. Eadie, and S. F. Goodwin.** 2010. Control of sexual differentiation and behavior by the doublesex gene in *Drosophila melanogaster*. *Nat Neurosci* **13**:458-66.
48. **Rogulja-Ortmann, A., J. Picao-Osorio, C. Villava, P. Patraquim, E. Lafuente, J. Aspden, S. Thomsen, G. M. Technau, and C. R. Alonso.** 2014. The RNA-binding protein ELAV regulates Hox RNA processing, expression and function within the *Drosophila* nervous system. *Development* **141**:2046-56.
49. **Salz, H. K.** 2011. Sex determination in insects: a binary decision based on alternative splicing. *Curr Opin Genet Dev* **21**:395-400.
50. **Samson, M. L.** 1998. Evidence for 3' untranslated region-dependent autoregulation of the *Drosophila* gene encoding the neuronal nuclear RNA-binding protein ELAV. *Genetics* **150**:723-33.
51. **Samson, M. L.** 2008. Rapid functional diversification in the structurally conserved ELAV family of neuronal RNA binding proteins. *BMC Genomics* **9**:392.
52. **Samson, M. L., and F. Chalvet.** 2003. found in neurons, a third member of the *Drosophila* elav gene family, encodes a neuronal protein and interacts with elav. *Mech Dev* **120**:373-83.
53. **Samuels, M. E., D. Bopp, R. A. Colvin, R. F. Roscigno, M. A. Garcia-Blanco, and P. Schedl.** 1994. RNA binding by Sxl proteins in vitro and in vivo. *Mol Cell Biol* **14**:4975-90.

54. **Schutt, C., and R. Nothiger.** 2000. Structure, function and evolution of sex-determining systems in Dipteran insects. *Development* **127**:667-77.
55. **Simionato, E., N. Barrios, L. Duloquin, E. Boissonneau, P. Lecorre, and F. Agnes.** 2007. The *Drosophila* RNA-binding protein ELAV is required for commissural axon midline crossing via control of commissureless mRNA expression in neurons. *Dev Biol* **301**:166-77.
56. **Soller, M.** 2006. Pre-messenger RNA processing and its regulation: a genomic perspective. *Cell Mol Life Sci* **63**:796-819.
57. **Soller, M., I. U. Haussmann, M. Hollmann, Y. Choffat, K. White, E. Kubli, and M. A. Schafer.** 2006. Sex-peptide-regulated female sexual behavior requires a subset of ascending ventral nerve cord neurons. *Curr Biol* **16**:1771-82.
58. **Soller, M., M. Li, and I. U. Haussmann.** 2008. Regulation of the ELAV target *ewg*: insights from an evolutionary perspective. *Biochem Soc Trans* **36**:502-4.
59. **Soller, M., and K. White.** 2004. *Elav*. *Curr Biol* **14**:R53.
60. **Soller, M., and K. White.** 2003. ELAV inhibits 3'-end processing to promote neural splicing of *ewg* pre-mRNA. *Genes Dev* **17**:2526-38.
61. **Soller, M., and K. White.** 2005. ELAV multimerizes on conserved AU4-6 motifs important for *ewg* splicing regulation. *Mol Cell Biol* **25**:7580-91.
62. **Stowers, R. S., and T. L. Schwarz.** 1999. A genetic method for generating *Drosophila* eyes composed exclusively of mitotic clones of a single genotype. *Genetics* **152**:1631-9.
63. **Thibault, S. T., M. A. Singer, W. Y. Miyazaki, B. Milash, N. A. Dompe, C. M. Singh, R. Buchholz, M. Demsky, R. Fawcett, H. L. Francis-Lang, L. Ryner, L. M. Cheung, A. Chong, C. Erickson, W. W. Fisher, K. Greer, S. R. Hartouni, E. Howie, L.**

- Jakkula, D. Joo, K. Killpack, A. Laufer, J. Mazzotta, R. D. Smith, L. M. Stevens, C. Stuber, L. R. Tan, R. Ventura, A. Woo, I. Zakrajsek, L. Zhao, F. Chen, C. Swimmer, C. Kopczynski, G. Duyk, M. L. Winberg, and J. Margolis.** 2004. A complementary transposon tool kit for *Drosophila melanogaster* using P and piggyBac. *Nat Genet* **36**:283-7.
64. **Toba, G., J. Qui, S. P. Koushika, and K. White.** 2002. Ectopic expression of *Drosophila* ELAV and human HuD in *Drosophila* wing disc cells reveals functional distinctions and similarities. *J Cell Sci* **115**:2413-21.
65. **Toba, G., and K. White.** 2008. The third RNA recognition motif of *Drosophila* ELAV protein has a role in multimerization. *Nucleic Acids Res* **36**:1390-9.
66. **Toba, G., D. Yamamoto, and K. White.** 2010. Life-span phenotypes of *elav* and *Rbp9* in *Drosophila* suggest functional cooperation of the two ELAV-family protein genes. *Arch Insect Biochem Physiol* **74**:261-5.
67. **Ule, J., G. Stefani, A. Mele, M. Ruggiu, X. Wang, B. Taneri, T. Gaasterland, B. J. Blencowe, and R. B. Darnell.** 2006. An RNA map predicting Nova-dependent splicing regulation. *Nature* **444**:580-6.
68. **Uren, P. J., S. C. Burns, J. Ruan, K. K. Singh, A. D. Smith, and L. O. Penalva.** 2012. Genomic analyses of the RNA-binding protein Hu antigen R (HuR) identify a complex network of target genes and novel characteristics of its binding sites. *J Biol Chem* **286**:37063-6.
69. **Venables, J. P., C. F. Bourgeois, C. Dalglish, L. Kister, J. Stevenin, and D. J. Elliott.** 2005. Up-regulation of the ubiquitous alternative splicing factor Tra2beta causes inclusion of a germ cell-specific exon. *Hum Mol Genet* **14**:2289-303.

70. **Wang, H., J. Molfenter, H. Zhu, and H. Lou.** 2010. Promotion of exon 6 inclusion in HuD pre-mRNA by Hu protein family members. *Nucleic Acids Res* **38**:3760-70.
71. **Wang, J., and L. R. Bell.** 1994. The Sex-lethal amino terminus mediates cooperative interactions in RNA binding and is essential for splicing regulation. *Genes Dev* **8**:2072-85.
72. **Yannoni, Y. M., and K. White.** 1999. Domain necessary for Drosophila ELAV nuclear localization: function requires nuclear ELAV. *J Cell Sci* **112**:4501-12.
73. **Yao, K.-M., M.-L. Samson, R. Reeves, and K. White.** 1993. Gene *elav* of *Drosophila melanogaster*: a prototype for neuronal-specific RNA binding protein gene family that is conserved in flies and humans. *J. Neurobiol.* **24**:723-739.
74. **Zanini, D., J. M. Jallon, L. Rabinow, and M. L. Samson.** 2012. Deletion of the Drosophila neuronal gene found in neurons disrupts brain anatomy and male courtship. *Genes Brain Behav* **11**:819-27.
75. **Zhu, H., M. N. Hinman, R. A. Hasman, P. Mehta, and H. Lou.** 2008. Regulation of neuron-specific alternative splicing of neurofibromatosis type 1 pre-mRNA. *Mol Cell Biol* **28**:1240-51.
76. **Zhu, H., H. L. Zhou, R. A. Hasman, and H. Lou.** 2007. Hu proteins regulate polyadenylation by blocking sites containing U-rich sequences. *J Biol Chem* **282**:2203-10.

Figure legends

Figure 1. Mutants of Drosophila ELAV family RBPs display distinct phenotypes, but converge in the regulation of synaptic growth.

(A-D) Axonal projections in control (A), *elav* (B, *elav^{e5}/Y*), *elav fne* (C, *elav^{e5} fne^Δ/Y*) and *elav fne Rbp9* (D, *elav^{e5} fne^Δ/Y; Rbp9^{P2690}*) embryos stained with Mab BP102. Arrowheads in B-D indicated projection defects and/or irregular positioning of neuromeres. The scale bar in A is 25 μm.

(E-L) Neuromuscular junctions at muscle 13 of control (E), *elav* (F, *elav^{e5}/elav^{ts1}*), *fne* (G, *fne^Δ/Df(1)ED7165*), *Rbp9* (H, *Rbp9^{P2690}/Df(2L)ED206*), *elav fne* (I, *elav^{e5} fne^Δ// elav^{ts1} fne^Δ*), *elav; RBP9* (J, *elav^{e5}/elav^{ts1}; Rbp9^{P2690}/Df(2L)ED206*) and *fne; Rbp9* (K, *fne^Δ/Df(1)ED7165; Rbp9^{P2690}/Df(2L)ED206*) third instar larvae stained with anti-HRP and quantification of type 1b boutons (L, n=15-30). The scale bar in E is 25 μm. *elav^{e5}/elav^{ts1}* mutants were raised at the permissive temperature during embryogenesis. Statistically significant differences compared to the control are indicated by stars (** p<0.01 and *** p<0.001).

(M-Q) Mushroom bodies of control (M), *elav* (N, *elav^{e5}/elav^{ts1}*, raised at the permissive temperature during embryogenesis), *fne* (O, *fne^Δ/Df(1)ED7165*), *Rbp9* (P, *Rbp9^{P2690}/Df(2L)ED206*) and *fne; Rbp9* (Q, *fne^Δ/Df(1)ED7165; Rbp9^{P2690}/Df(2L)ED206*) adult flies stained with anti-Fas2. Arrowheads in O and Q indicated fused beta lobes. The scale bar in M is 25 μm.

(R-V) Photoreceptors of control (R), *elav* (S, *elav^{e5}* whole eye clone), *fne* (T, *fne^Δ/Df(1)ED7165*), *Rbp9* (U, *Rbp9^{P2690}/Df(2L)ED206*) and *fne RBP9* (V, *fne^Δ/Df(1)ED7165;*

Rbp9^{P2690}/Df(2L)ED206) adult flies from paraffin sections visualized by auto-fluorescence. The scale bar in R is 5 μ m.

(W-AB) Horizontal paraffin sections of adult heads from control (W), *fne* (X, *fne^Δ/Df(1)ED7165*), *Rbp9* (Y, *Rbp9^{P2690}/Df(2L)ED206*) and *fne; Rbp9* (Z, *fne^Δ/Df(1)ED7165; Rbp9^{P2690}/Df(2L)ED206*) 40 d old adult flies and from *elav* (*elav^{e5}/elav^{ts1}*, raised at the permissive temperature during embryogenesis) 1 d (AA) and 7 d (AB) old adult flies visualized by auto-fluorescence. Arrowheads in Z, AA and AB indicated vacuolization, and the star in AA and AB indicates the non-rotated medulla. The scale bar in W is 50 μ m.

(AC) Longevity of control, *elav* (*elav^{e5}/elav^{ts1}*, raised at the permissive temperature during embryogenesis), *fne* (*fne^Δ/Df(1)ED7165*), *Rbp9* (*Rbp9^{P2690}/Df(2L)ED206*) and *fne; Rbp9* (*fne^Δ/Df(1)ED7165; Rbp9^{P2690}/Df(2L)ED206*) is shown as mean from 3 replicates (20 flies each) with the standard error.

(AD) Negative geotaxis of 1 d, 10 d and 20 d old *elav* (*elav^{e5}/elav^{ts1}*, raised at the permissive temperature during embryogenesis), *fne* (*fne^Δ/Df(1)ED7165*), *Rbp9* (*Rbp9^{P2690}/Df(2L)ED206*) and *fne; Rbp9* (*fne^Δ/Df(1)ED7165; Rbp9^{P2690}/Df(2L)ED206*) adult flies are shown as mean from 3 experiments with the standard error normalized to the performance of control flies (set to 100%). Statistically significant differences of comparisons to control flies are indicated by stars above the column or within genotype with brackets (***) $p < 0.001$).

Figure 2. Loss of FNE and RBP9 does not affect alternative splicing of ELAV target genes *erect wing*, *neuroglian* and *armadillo*.

(A) Analysis of neuronal alternative splicing in the *ewg*, *nrg* and *arm* genes in *fne; Rbp9* double mutants by RT-PCR. n: neuronal isoform, c: canonical isoform.

(B) Schematic of the ELAV responsive *nrg* GFP reporter *UNGA*.

(C-E). Alternative splicing of *nrg* from the *UNGA* reporter visualized by anti-GFP staining is not affected in photoreceptor neurons of *fne; Rbp9* mutants, but dramatically reduced in *elav^{edr}* mutants. The scale bar is 50 μ m.

(F-I) Alternative splicing of *nrg* from the *UNGA* reporter is not affected in neurons of the 3rd instar larval or adult brain in *fne; Rbp9* mutants visualized with anti-GFP staining (top row) and compared to anti-ELAV staining (middle and bottom row). Note the complete overlap between ELAV expression and GFP from the spliced *UNGA* reporter in *fne; Rbp9* mutants (bottom row F-I). The scale bars are 100 μ m.

Figure 3. Binding of recombinant ELAV/Hu family RBPs to RNA of the ELAV target *ewg*.

(A) SDS-polyacrylamide gel showing Coomassie blue stained recombinant ELAV family RBPs used for binding assays. For each of the recombinant proteins, 0.5 μ g, 1 μ g and 2 μ g were loaded. Marker proteins were bovine serum albumin (66 kDa), ovalbumin (45 kDa) and carbonic anhydrase (30 kDa). A bacterial protein co-purifying with rFNA is indicated by a star in lanes 7-9.

(B) EMSA gel with RNA from the ELAV binding site in *ewg* (pA2-I). Uniformly ³²P-labeled RNAs (100 pM) were incubated with recombinant proteins (2 nM, 8 nM, 32 nM, 125 nM, 500 nM) and separated on 4% native polyacrylamide gels.

(C) Graphic representation of EMSA data. The percent of bound RNA (input RNA-unbound RNA/input RNA x 100) is plotted against the concentration of recombinant proteins (in M) presented as log.

Figure 4. Elevated levels of FNE, RBP9 and HuR can regulate alternative splicing of ELAV targets.

(A) Expression of HA-tagged ELAV, FNE, RBP9 and HuR from *UAS* containing transgenes in adults with *nsybGAL4* by Western blot detection with anti-ELAV antibodies.

(B) Neuronal alternative splicing of ELAV targets *ewg* intron 6 from exon H to J, *nrg* and *arm* induced by expression of HA-tagged ELAV, FNE, RBP9 and HuR from *UAS* containing transgenes in wing discs with *dppGAL4* assessed by RT-PCR. c: canonical, n: neuronal

(C-I) Neuronal alternative splicing of the *nrg* GFP reporter *UNGA* upon expression of HA-tagged ELAV, FNE, RBP9 and HuR from *UAS* containing transgenes in wing discs with *dppGAL4*. The upper row in D-G shows staining with anti-GFP, the middle row staining with anti-HA and the lower row merged pictures. Due to temporally regulated expression of *dppGAL4* and because expression of ELAV proteins precedes GFP expression, signals of ELAV proteins and GFP do not entirely overlap. Note that the distantly related polyU binding protein Hfp (H) and the SR protein B52 (I) do not induce *UNGA* splicing. The scale bar in I is 150 μm .

(J-M) Cellular localization of HA-tagged ELAV, FNE, RBP9 and HuR from *UAS* containing transgenes in wing discs with *dppGAL4*. The upper row shows staining with anti-HA, the middle row nuclei stained with DAPI and the lower row merged pictures. The scale bar in M is 10 μm .

(N-S) Neuronal alternative splicing of the *nrg* GFP reporter *UNGA* upon expression of HA-tagged ELAV, FNE, RBP9 and HuR from *UAS* containing transgenes in wing discs with *dppGAL4* in the presence of temperature-sensitive inhibitor of GAL4, GAL80^{ts}, expressed from a *UAS* transgene at 18°C (N), 25°C (O and Q-S) and 29°C (P). The upper row in N-P shows staining with anti-GFP, the middle row staining with anti-HA and the lower row in N-P and in Q-S merged pictures. The scale bar in S is 150 μm .

(T) Quantification of *UNGA*-splicing shown as means with the standard error from five wing discs.

Figure 5. Rescue of eye development by ELAV/Hu family RBPs in *elav* mutant eyes

(A) Schematic of the *eFVGU elav* rescue construct. FRT mediated recombination results in loss of *elav* and *GAL4* expression under the *elav* promoter.

(B-D) Eye and eye discs of *elav^{es} eFVGU; eyflp* males. Neurons in C and D are stained with anti-ELAV and MAb 24B10, respectively.

(E-J) Eyes of wild type and *elav^{es} eFVGU; eyflp* males expressing ELAV/Hu family RBPs or Sxl from *UAS* transgenes.

(K) Quantification of the eye size (in μm^2) shown in B and E-J. Statistically significant rescue compared to the absence of a *UAS* transgene is indicated by stars (***) $p < 0.001$.

Figure 6. FNE, RBP9 and HuR can replace neuronal ELAV function under the control of the *elav* gene.

(A) Schematic of the *elav* rescue construct *elavHAELAV*.

(B) Expression of HA-tagged ELAV, FNE, RBP9 and HuR under the control of the *elav* gene in adult flies by Western blot detection with anti-HA antibodies. In lane two, HAELAV has a larger size due to the presence of the HA-tag.

(C) Rescue of adult viability of strong hypomorph *elav^{ts1}* by expression of HA-tagged ELAV, FNE, RBP9, HuR and NLSRBP9 under the control of the *elav* gene. n=200-400.

(D) Rescue of synaptic growth in *elav^{es}/elav^{ts1}* by expression of HA-tagged ELAV, FNE, RBP9 and HuR under the control of the *elav* gene raised at the permissive temperature during

embryonic development is shown as mean with the standard error of type 1b boutons at muscle 13 (n=15-28).

(E-S) Cellular localization of HA-tagged ELAV, FNE, RBP9, HuR and NLSRBP9 under the control of the *elav* gene in larval ventral nerve cord midline neurons. The left column shows staining with anti-HA, the middle column nuclei stained with DAPI or anti-ELAV and the right column merged pictures. Arrow heads in Q and R point towards neurons, where NLSHARBP9 is predominantly nuclear, while ELAV becomes cytoplasmic. The scale bar in P is 10 μm .

Figure 7. Sxl induced alternative splicing of ELAV target *nrg* and interference ELAV family RBPs with sexual differentiation and dosage compensation.

(A-C) Neuronal alternative splicing of the *nrg* GFP reporter *UNGA* in control wing discs and upon expression of *UASHAELAV* or *UASSxl* with *dppGAL4* stained with anti-GFP antibodies. The scale bar in C is 150 μm .

(D-I) Expression of ELAV with *dsxGAL4* inhibits sexual differentiation of male genitals (side and back view in D, E and in F, G) and sex combs (H and I). Scale bars in E and G are 100 μm , and in I 50 μm .

(J) Viability of males from neuronal over-expression of *UAS* transgenes with *elavGAL4^{C155}* shown as percentage relative to females from the same cross. Total number of flies is shown in brackets.

(K) Viability of females from crosses of mutants in ELAV family proteins with *Sxl^{7B0}* null males shown as percentage relative to balancer carrying females (*elav*) or to males (*fne* and *Rbp9*) from the same cross. Total number of flies is shown in brackets.

Figure 8. Model for target selectivity and functional diversification of ELAV/Hu family RBPs. Circles represent the complement of targets for ELAV, FNE and RBP9, and overlapping areas indicate shared targets. Main determinants of target selectivity are concentration, binding activity and sub-cellular localization.

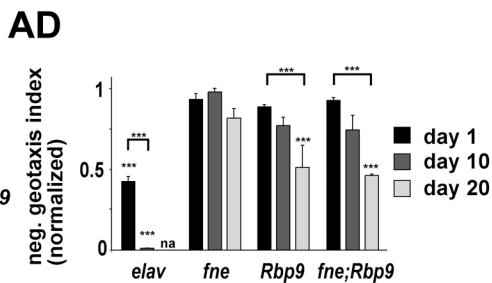
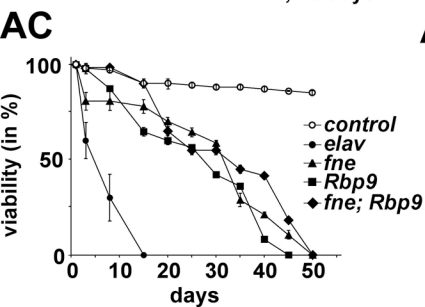
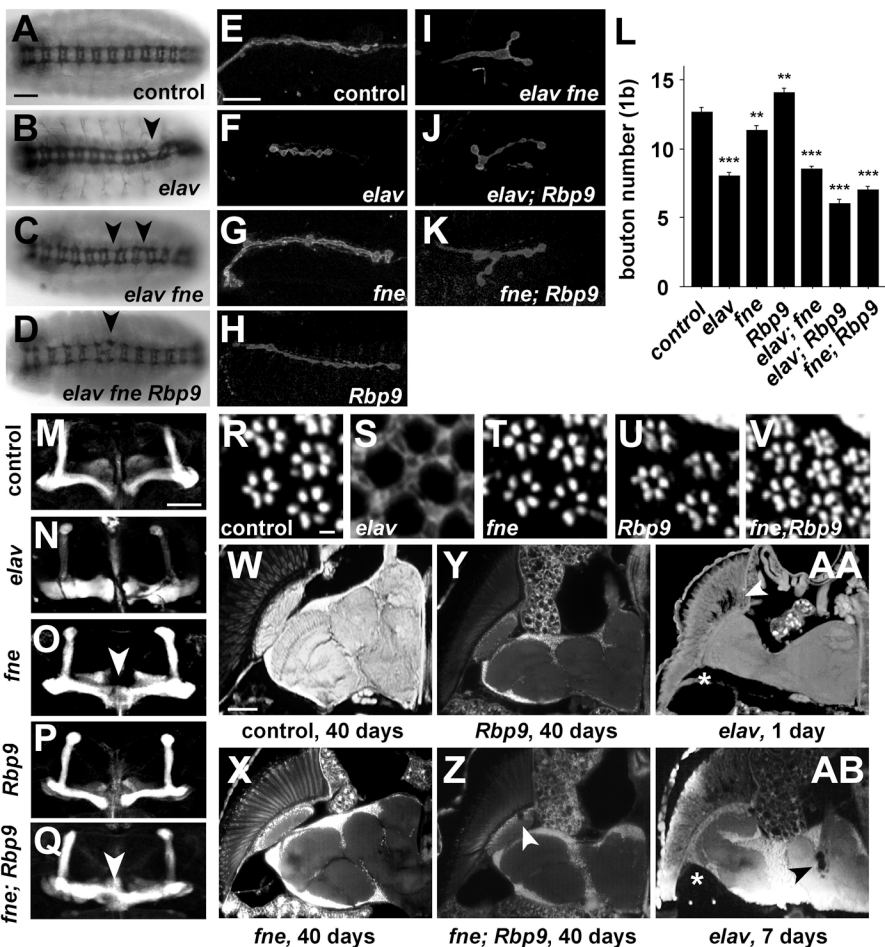


Figure 3

Zaharieva et al.

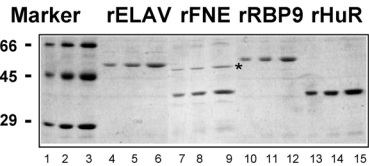
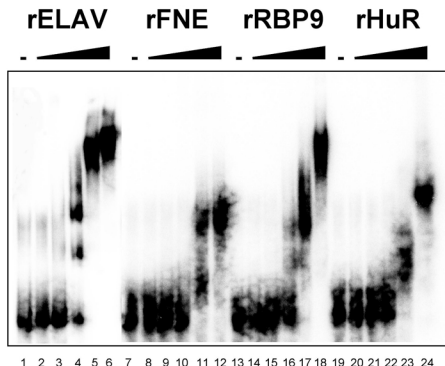
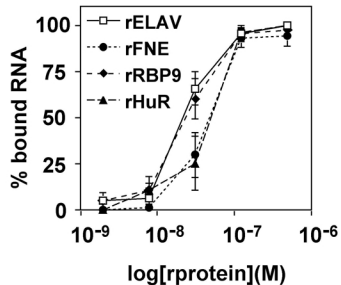
A**B****C**

Figure 4
Zaharieva et al.

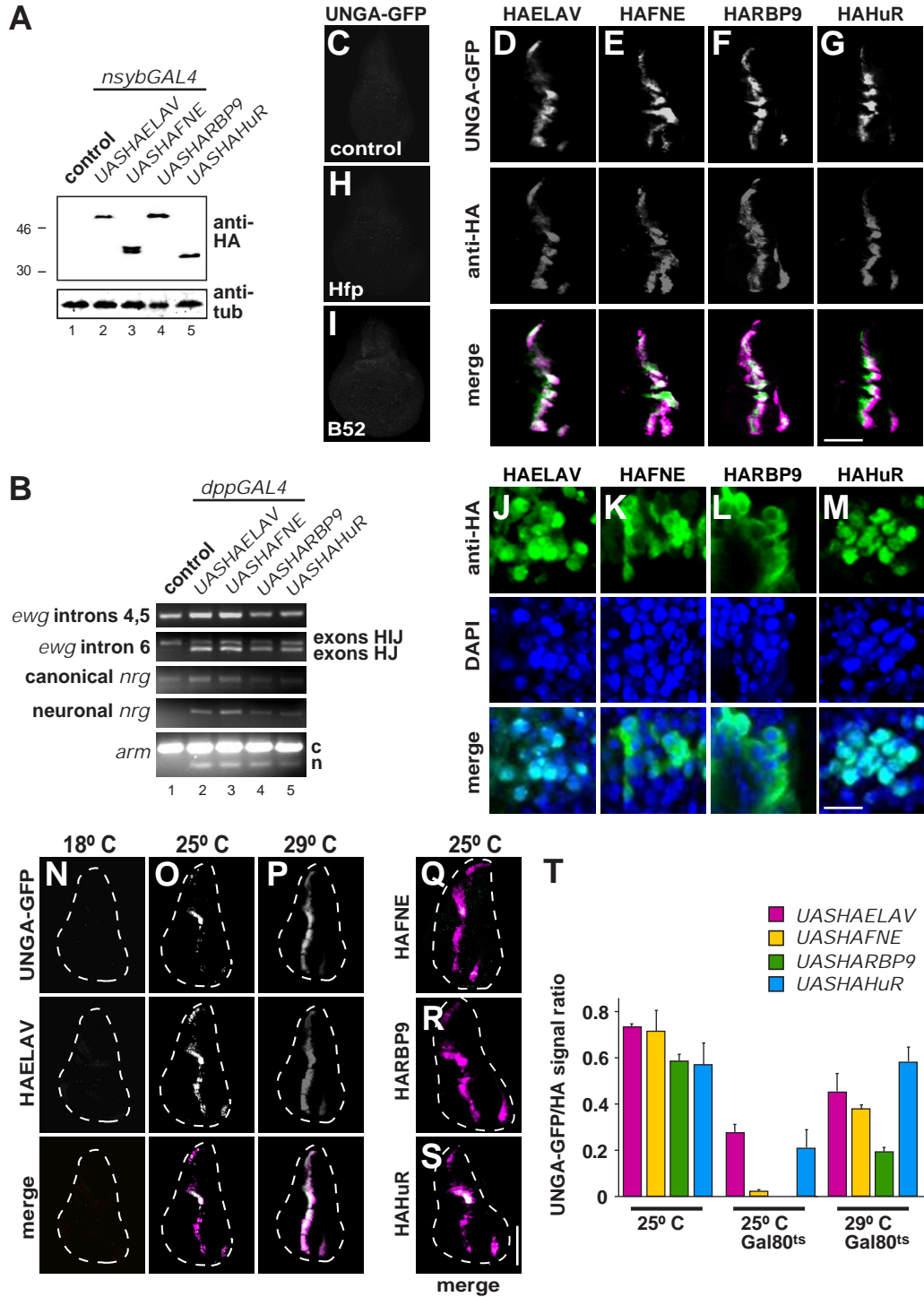


Figure 5
Zaharieva et al.

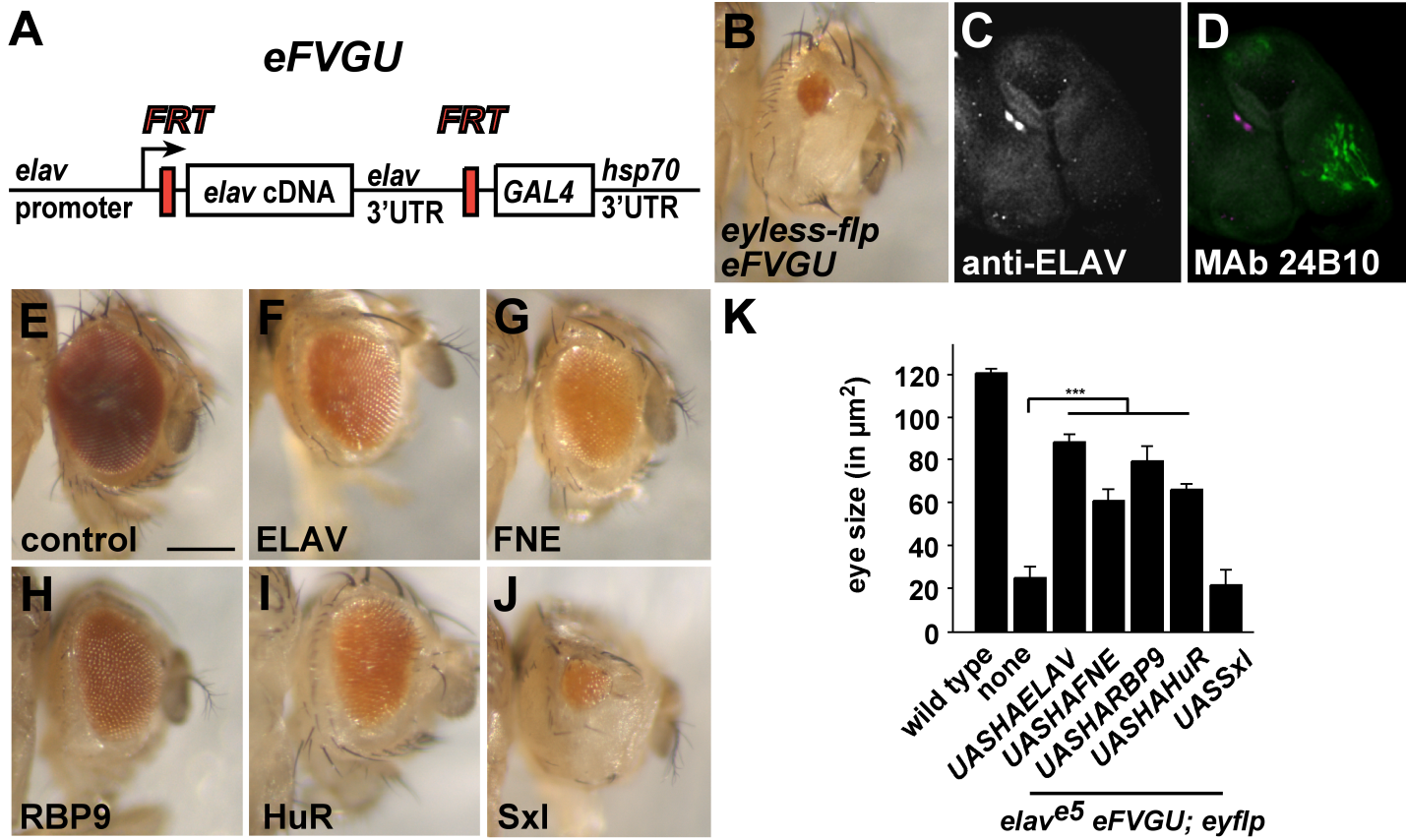
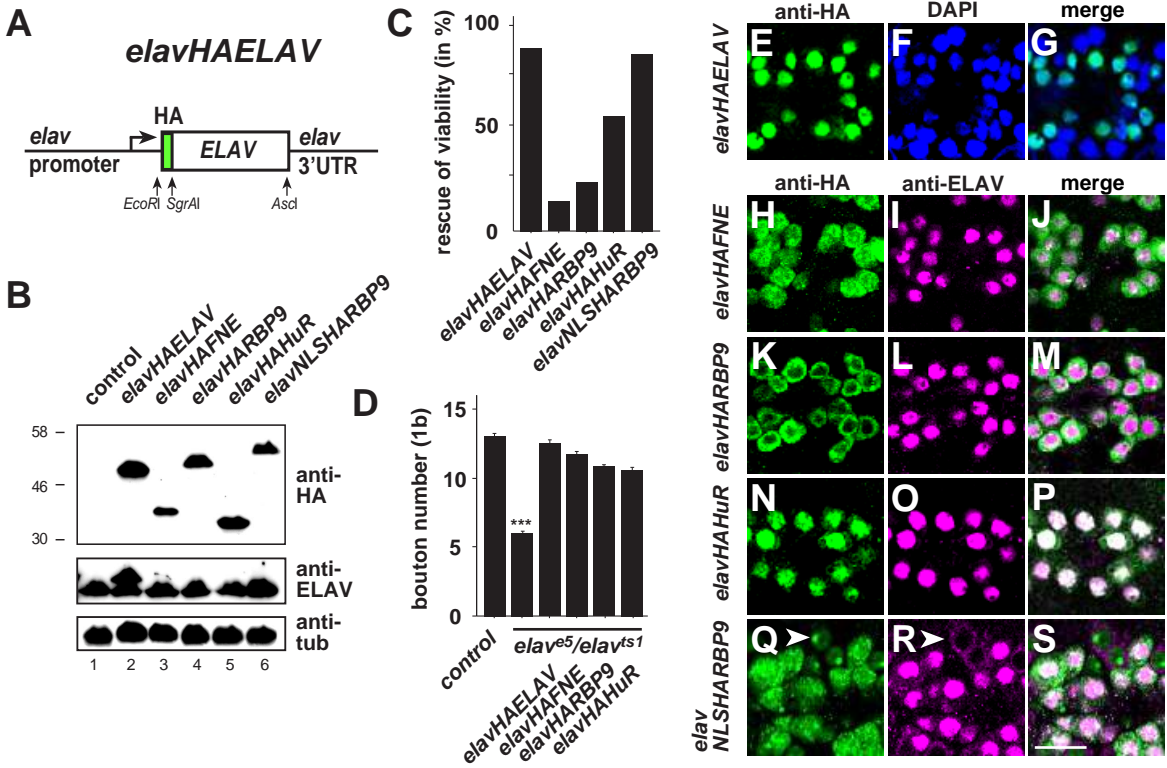
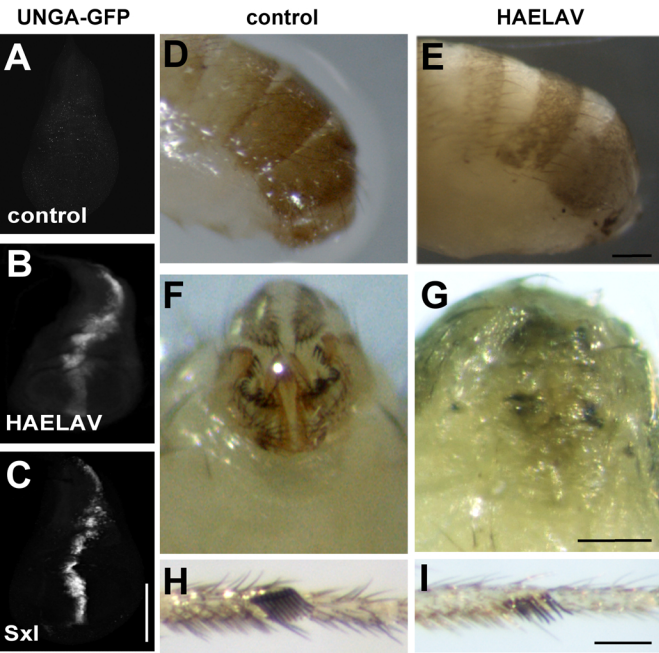


Figure 6
Zaharieva et al.





J

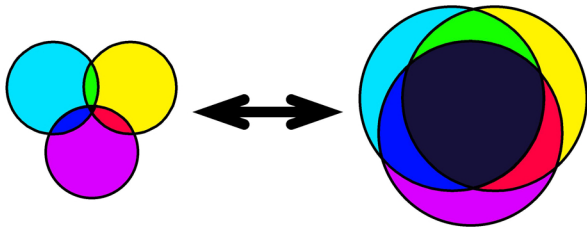
		males
C155Gal4	none	88 % (127)
	UASHAELAV	66 % (88)
	UASHAELAV ^{OH}	7 % (82)
	UASHAFNE	4 % (76)
	UASHARBP9	0 % (60)
	UASHANLSRBP	105 % (123)
	UASHAHuR	lethal in both sexes
	UASSxl	17 % (104)

K

cross	female progeny	
	+/ <i>Sxl</i> ^{null} +/+	+/ <i>Sxl</i> ^{null} +/ <i>elav</i> ^{null} , <i>fne</i> ^{null} or <i>RBP9</i> ^{null}
<i>elav</i> ^{null} / <i>FM7</i>	100 %	115 % (201)
<i>fne</i> ^{null} / <i>fne</i> ^{null}	n.d.	102 % (456)
<i>RBP9</i> ^{null} / <i>CyO</i>	9 %	7 % (564)

Sxl^{null} males crossed with

Figure 8
Zaharieva et al.

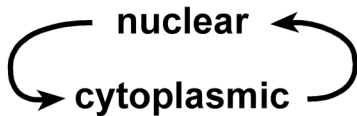


concentration
activity

low
low

high
high

localization



Concentration and localization of co-expressed ELAV/Hu proteins control specificity of mRNA processing

EMANUELA ZAHARIEVA, IRMGARD U. HAUSSMANN, ULRIKE BRÄUER AND MATTHIAS SOLLER

Supplemental table and figure legends

Table S1. Sequence identity (similarity) in RRM1-3 among *Drosophila* ELAV RBPs and compared to human Hu RBPs and Sex lethal (Sxl).

Figure S1. ELAV, FNE and RBP9 are co-expressed in neurons.

(A and B) Expression of FNE in adult brains of transgenes harboring an HA-epitope-tagged genomic construct stained with anti-HA antibodies (top row) in the absence of endogenous FNE and ELAV stained with anti-ELAV antibodies (middle row). Note that expression of FNE completely overlaps with ELAV (bottom row), but that FNE localizes to both nucleus and cytoplasm, while ELAV is mostly nuclear. Scale bars are 100 μm in A and 30 μm in B.

(C and D) Expression of RBP9 in adult brains of transgenes harboring an myc-epitope-tagged genomic construct stained with anti-myc antibodies (top row) in the absence of endogenous RBP9 and ELAV stained with anti-ELAV antibodies (middle row). Note that expression of RBP9 completely overlaps with ELAV (bottom row), but that RBP9 localizes to the cytoplasm, while ELAV is mostly nuclear. Scale bars are 100 μm in A and 30 μm in B.

Figure S2. Generation of an *fne* null allele.

(A) Genomic organization of the *fne* locus. A deletion of the *fne* coding region was obtained by flipase mediated recombination of the FRT sites contained within PBac transposons.

(B) Genomic PCR amplifying the 5' (top) and 3' (middle) flanking region and RT-PCR (bottom) of parental transposons and two identical deletion lines.

Figure S3. Loss of FNE or RBP9 does not affect alternative splicing of *nrg* from the *UNGA* reporter.

(A-D). Alternative splicing of *nrg* from the *UNGA* reporter is not affected in photoreceptor neurons of *fne* or *Rbp9* mutants stained with anti-GFP antibodies, but dramatically reduced in *elav^{edr}* mutants. The scale bar is 50 μm .

(E-G) Alternative splicing of *nrg* from the *UNGA* reporter is not affected in neurons of the 3rd instar larval brain in *fne* or *Rbp9* mutants visualized by GFP expression. The scale bars are 100 μm .

Figure S4. Expression and regulation of the *UNGA* reporter by Hu RBPs.

(A-O) HA-tagged ELAV and Hu proteins were expressed from *UAS* constructs in wing discs using *dppGAL4* in the presence of the *nrg* alternative splicing reporter *UNGA* and stained with anti-GFP antibodies and anti-HA antibodies. Note that HuD could not be detected although its expression results in lethality when expressed with *elavGAL4^{C155}*. The scale bar in O is 150 μm .

(P) Quantification of *UNGA* splicing showing means with the standard error from 4 wing discs.

Figure S5. Expression of *elav*, *fne* and *Rbp9* during development and in adults determined by RNAseq from flybase. Sexually dimorphic expression in adults is shown by dashed lines.

Supplemental Table S1

RRM1

	ELAV	FNE	RBP9
ELAV	-	81(93)	78(89)
FNE	-	-	80(90)
HuR	77(88)	81(90)	78(86)
HuB	73(90)	81(91)	78(89)
HuC	69(85)	73(86)	73(84)
HuD	75(89)	82(90)	80(87)
Sxl	49(74)	51(73)	49(73)

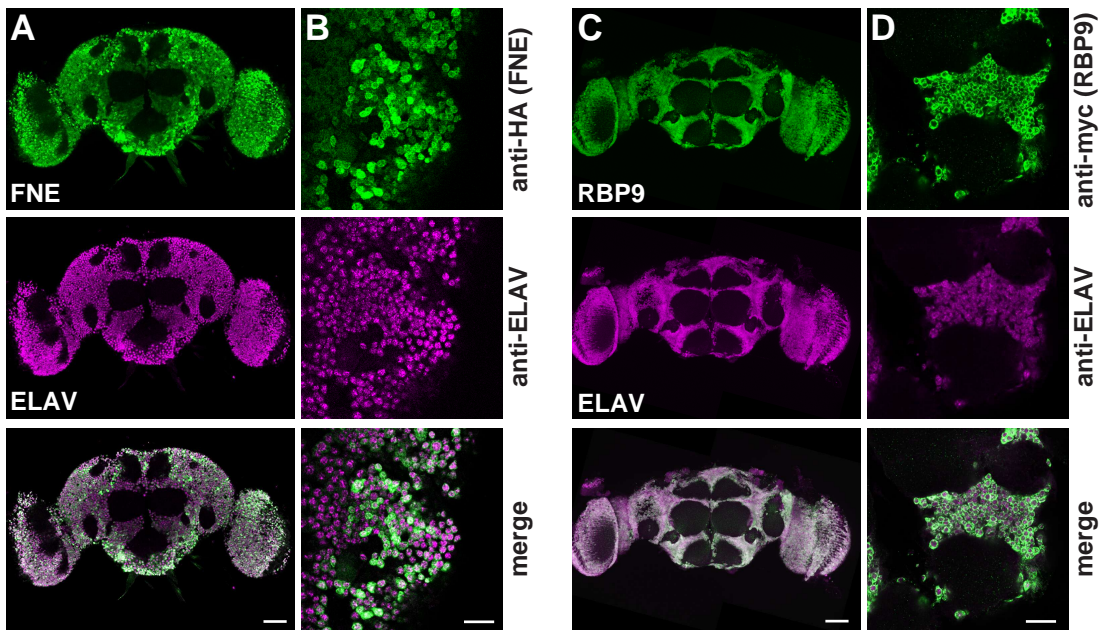
RRM2

	ELAV	FNE	RBP9
ELAV	-	63(76)	66(80)
FNE	-	-	82(90)
HuR	52(70)	63(77)	64(76)
HuB	61(73)	66(82)	73(82)
HuC	58(72)	67(84)	69(81)
HuD	63(75)	66(82)	73(82)
Sxl	41(64)	41(64)	41(65)

RRM3

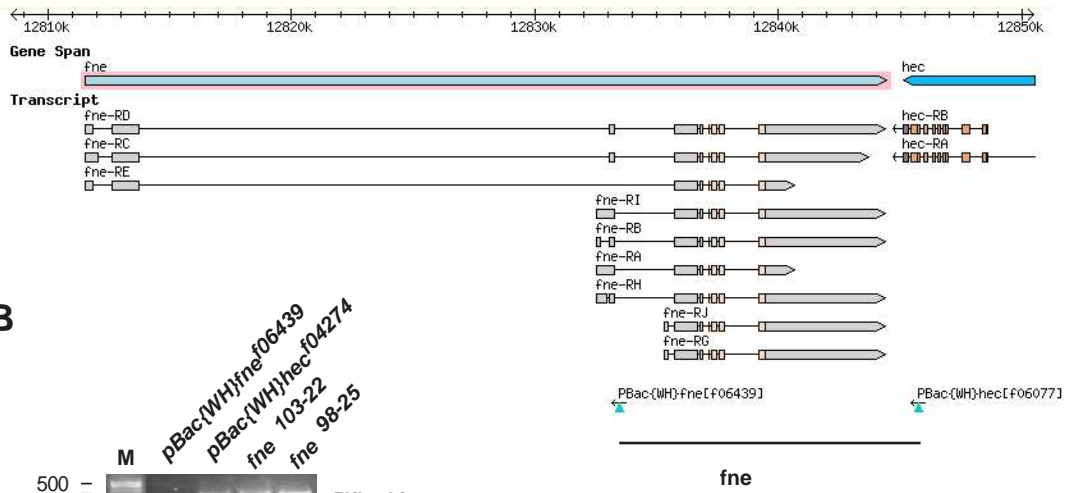
	ELAV	FNE	RBP9
ELAV	-	75(90)	72(90)
FNE	-	-	80(98)
HuR	63(84)	71(86)	73(86)
HuB	67(86)	80(90)	78(89)
HuC	67(86)	78(86)	76(86)
HuD	69(89)	80(90)	80(90)

Supplemental Figure 1

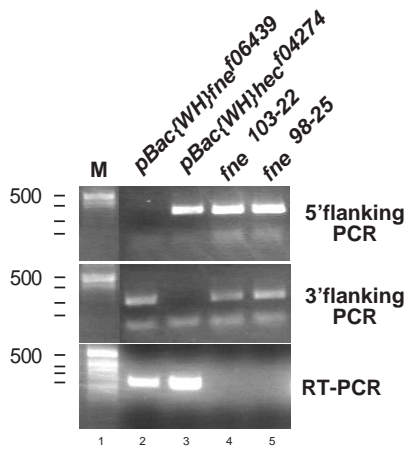


Supplemental Figure 2

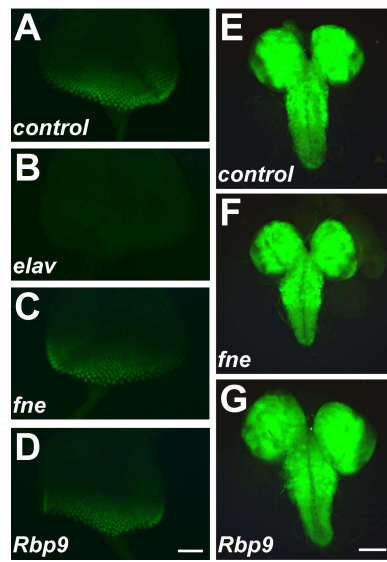
A



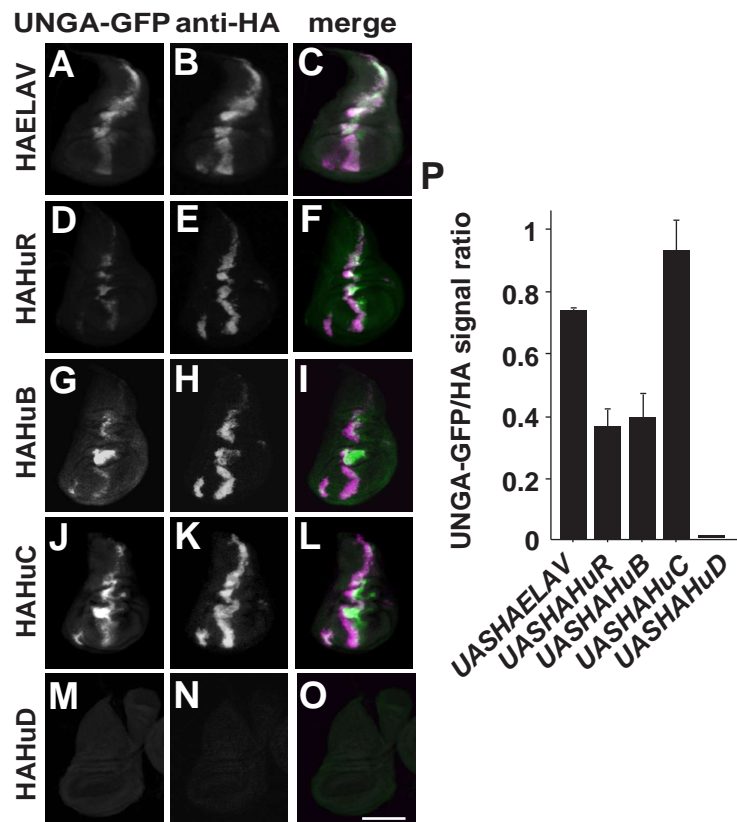
B



Supplemental Figure 3



Supplemental Figure 4



Supplemental Figure 5

